



CHORUS

This is the accepted manuscript made available via CHORUS. The article has been published as:

Driving magnetic order in a manganite by ultrafast lattice excitation

M. Först, R. I. Tobey, S. Wall, H. Bromberger, V. Khanna, A. L. Cavalieri, Y.-D. Chuang, W. S. Lee, R. Moore, W. F. Schlotter, J. J. Turner, O. Krupin, M. Trigo, H. Zheng, J. F. Mitchell, S. S.

Dhesi, J. P. Hill, and A. Cavalleri

Phys. Rev. B **84**, 241104 — Published 2 December 2011

DOI: [10.1103/PhysRevB.84.241104](https://doi.org/10.1103/PhysRevB.84.241104)

Driving magnetic order in a manganite by ultrafast lattice excitation

M. Först^{1*}, R.I. Tobey^{2*}, S. Wall^{3*}, H. Bromberger¹, V. Khanna^{1,4,11}, A.L. Cavalleri¹,
Y.-D. Chuang⁵, W.S. Lee⁶, R. Moore⁶, W.F. Schlotter⁷, J.J. Turner⁷, O. Krupin⁸, M. Trigo⁹,
H. Zheng¹⁰, J.F. Mitchell¹⁰, S.S. Dhesi¹¹, J.P. Hill², A. Cavalleri^{1,4#}

¹*Max-Planck Department for Structural Dynamics, Center for Free Electron Laser Science,
University of Hamburg, Germany*

²*Condensed Matter Physics and Materials Science Department,
Brookhaven National Laboratory, Upton, NY*

³*Fritz-Haber-Institute of the Max Planck Society, Berlin, Germany*

⁴*Department of Physics, Clarendon Laboratory, University of Oxford, United Kingdom*

⁵*Advanced Light Source, Lawrence Berkeley Laboratory, Berkeley, CA*

⁶*SIMES, SLAC National Accelerator Laboratory and Stanford University, Menlo Park, CA*

⁷*Linac Coherent Light Source, SLAC National Accelerator Laboratory, Menlo Park, CA*

⁸*European XFEL, Hamburg, Germany*

⁹*PULSE, SLAC National Accelerator Laboratory, Menlo Park, CA*

¹⁰*Materials Science Division, Argonne National Laboratory, Argonne, IL*

¹¹*Diamond Light Source, Chilton, Didcot, Oxfordshire, United Kingdom.*

* These authors contributed equally to this work.

Corresponding authors: michael.foerst@mps.dcfel.de, andrea.cavalleri@mps.dcfel.de

Abstract

Femtosecond mid-infrared pulses are used to directly excite the lattice of the single-layer manganite $\text{La}_{0.5}\text{Sr}_{1.5}\text{MnO}_4$. Magnetic and orbital orders, as measured by femtosecond resonant soft x-ray scattering with an x-ray free electron laser, are reduced within few picoseconds. This effect is interpreted as a *displacive exchange quench*, a prompt shift in the equilibrium value of the magnetic and orbital order parameters after the lattice has

been distorted. Control of magnetism through ultrafast lattice excitation may serve as a new paradigm for high-speed optomagnetism.

Ultrafast optical control of magnetism, of interest for high-speed data processing and storage, has to date only been demonstrated with near-infrared excitation. In highly absorbing materials, e.g., metals and semimetals, these photons of eV energy significantly heat the electronic and/or lattice systems to induce spin flips on the meV energy scale [1,2,3], and the stimulation is accompanied by strong dissipation. In complex oxides, where the physics at hand are strongly tied to the complex interplay of spin, charge and orbital degrees of freedom, near-IR excitation to switch the magnetic phase state [4] can be understood as the transfer of charges across semicovalent bonds, which perturbs orbital occupancy and thus drastically affects the exchange interactions [5,6].

An alternative path to steer condensed matter on the ultrafast time scale is the coherent optical excitation of lattice vibrations in the mid-infrared, which has been shown to control the electronic transport properties of complex oxides [7,8,9]. To aid understanding this vibrational control between insulating, metallic or superconducting phases, we have recently unraveled the microscopic mechanism of the coherent lattice excitation, namely ionic Raman scattering, which exerts a directional force onto the crystal structure via lattice anharmonicities [10]. In manganites, magnetism is also directly coupled to the lattice, as evidenced by the response to external and chemical pressure [11,12], or to ferroelectric polarization [13,14,15]. The deformation of the bonding geometry and the corresponding change in hopping amplitude is capable of modifying the electronic and magnetic order in the spirit of the exchange interactions described by the Goodenough-Kanamori-Anderson rules [16]. Thus, coherent lattice excitation at energies of tens of meV may open up new possibilities for low-dissipative ultrafast control of magnetic order, although an experimental verification is still

lacking. And it is not excluded that bond selective deformations may be applied to steer condensed matter phases in two directions, of great interest for switching applications.

In this work, we use femtosecond mid-infrared pulses to excite the lattice in half-doped $\text{La}_{0.5}\text{Sr}_{1.5}\text{MnO}_4$, inducing dynamics of spin and orbital order that are measured by femtosecond resonant soft x-ray scattering with an x-ray free electron laser. We observe that these electronic orders are reduced within different time constants in the few-picosecond range, and interpret this as the relaxation of the free energy following a *displacive exchange quench* through nonlinear rectification of the resonantly driven vibrational field. We compare these results to the case of near-infrared excitation, which predominantly photo-dopes the correlated compound. This enables us to distinguish the importance of cooperative Jahn-Teller distortions and exchange interactions for vibrational excitation.

At low temperatures ($T < T_N=110 \text{ K} < T_{CO/OO}=220 \text{ K}$), the single-layered $\text{La}_{0.5}\text{Sr}_{1.5}\text{MnO}_4$ compound exhibits CE-type charge, spin and orbital order, characterized by “zig-zag” ferromagnetic chains in the (001) planes, antiferromagnetically coupled with one another, in and out of these planes [17,18,19]. Resonant soft X-ray diffraction at the $2p \rightarrow 3d$ transitions (Mn $L_{2,3}$ edges) is directly sensitive to this spin and orbital order, providing both momentum-dependent and spectroscopic information [20,21]. Figure 1(a) shows the top-view of the relevant scattering geometries at the orbital $(\frac{1}{4} \frac{1}{4} 0)$ and the magnetic $(\frac{1}{4} \frac{1}{4} \frac{1}{2})$ wave vectors for a $\text{La}_{0.5}\text{Sr}_{1.5}\text{MnO}_4$ crystal cut with a (110) surface normal. Static energy scans at the Mn L_3 and L_2 edges, also displayed, are in agreement with the literature [22, 23].

In our experiments, $\text{La}_{0.5}\text{Sr}_{1.5}\text{MnO}_4$ was held at a base temperature of 25 K, and excited by 130-fs 1.2-mJ/cm^2 mid-infrared pulses, obtained by difference-frequency mixing of the signal and idler output from an infrared optical parametric amplifier. These pulses, polarized in the *ab*-plane of the

sample, were tuned to a centre wavelength of 13.5 μm (92 meV) with a 4.5- μm FWHM bandwidth, covering the 16- μm (78 meV) Mn-O stretching vibration [24]. Pulses at this wavelength were previously shown to excite the lattice and perturb electronic order in $\text{La}_{0.5}\text{Sr}_{1.5}\text{MnO}_4$ [8].

The excitation pulse train was synchronized to the 60-Hz repetition rate of the LCLS, an X-ray free electron laser (FEL) [25], which was operated at 640 eV in the 40-pC low-charge mode with sub-30 fs pulse duration. Femtosecond Resonant Soft X-ray Diffraction [6,26] at the Mn L_3 edge was used to probe orbital and magnetic order dynamics with 250-fs time resolution, limited by the timing jitter between the mid-infrared and x-ray pulses. The diffracted light was detected for each time delay with a fast-readout CCD camera, recording images individually at 60 Hz. The diffraction spots for the two different scattering geometries, oriented in such a way that the scattering plane of the experiment is horizontal, are shown in Fig. 1(b) and (c). Transient changes in spot intensity, position, and width were evaluated by fitting Lorentzian profiles to the data (red solid lines).

The temporal evolution of the integrated diffraction spot intensity at the magnetic $(\frac{1}{4} \frac{1}{4} \frac{1}{2})$ wave vector is reported in Figure 2(a). Diffraction was reduced by 8%, with a single time constant of 12.2 ps. For comparison, we display the significantly faster response measured after excitation with 5-mJ/cm² pulses at 800-nm wavelength [27,28], which reveals a prompt collapse of magnetic order on the 250 fs time resolution of the experiment. We re-iterate here that the disordering of the antiferromagnetic state for electronic excitation in the near-infrared is determined by the instantaneous charge transfer across semicovalent bonds [4,5,6], and thus is expected to follow the temporal shape of the laser pulse. The observation of a different timescale for the lattice-driven magnetic disordering is then evidence that this stimulation must be followed by a different physical path.

In Figure 2(b), we display the orbital order dynamics measured at the $(\frac{1}{4} \frac{1}{4} 0)$ diffraction peak after mid-infrared excitation. The transient responses of the orbital and magnetic peaks differ both in the timescale and amplitude, with the orbital order only reduced by only 3% with a single-exponential decay time of 6.3 ps. We note that this lattice-driven orbital disordering is slower than was observed previously by time-dependent optical birefringence [8,24], which however is a less direct method than the resonant x-ray diffraction used here.

Throughout these dynamics, we see no transient change in the position and width of the scattered diffraction spots for either order, and conclude that the correlation lengths are not perturbed. This is shown in Figure 2(c) where we plot the transient width of the magnetic diffraction spot together with its peak position. The latter is constant within $< 1 \times 10^{-5}$ (calculated standard deviation). For a thermal expansion coefficient of $6 \times 10^{-6} \text{ K}^{-1}$ [29] this corresponds to a temperature increase of less than 2 K, indicative of the low dissipation and non-thermal character associated with this vibrational excitation. This number is in agreement with a calculated upper limit of 2 K temperature increase for a 2-mJ/cm² excitation on the phonon resonance (see Ref. 8 for details) [30]. In addition, the different time scales of the orbital and magnetic order melting, as shown in Fig. 2(a), support a non-thermal driving mechanism for the observed dynamics. Light-induced heating of the sample across the Neel temperature T_N and the charge/orbital ordering temperature $T_{CO/OO}$ would result in a faster response of the magnetic compared to the orbital order response, which is opposite of what we observe here.

Recently, lattice dynamics observed in $\text{La}_{0.7}\text{Sr}_{0.3}\text{MnO}_3$ following mid-infrared excitation have been explained in terms of *Ionic Raman scattering* (IRS) [10,31,32]. The key step of IRS is the resonant excitation of a large amplitude infrared-active vibration, whose mechanical field is rectified through the second-order lattice polarizability – a process analogous to rectification in nonlinear optics. If Q_{IR} is the normal coordinate of the infrared-active vibration, its rectification leads to a half cycle force

field along the coordinate defined by the product symmetry group $Q_{IR} \bullet Q_{IR}$. Importantly, this half cycle field tends a finite area, resulting in a displacive force that leaves the lattice in a new position at the end of the pulse. The displacement has amplitude proportional to Q_{IR}^2 and Raman symmetry [10]. In Figure 3(a) we show a schematic of the low-temperature charge- and orbital-order unit cell of $\text{La}_{0.5}\text{Sr}_{1.5}\text{MnO}_4$ [33], which belongs to the D_{2h} point group. The 630-cm^{-1} ($16\text{-}\mu\text{m}$) stretching mode excited by the mid-infrared light field [24,34] has B_{2u} symmetry (see Figure 3(b)) [35], while the rectified field belongs to the product group $B_{2u} \otimes B_{2u} = A_g$, among which we find the Raman-active Jahn-Teller mode shown in Fig. 3(c). Thus, according to the IRS model, rectification of the mid-infrared mode relaxes the cooperative Jahn-Teller distortion. We conjecture that this reduces the splitting between crystal field levels and likely melts the ordering of the orbitals, weakening also the exchange interaction.

We stress that in contrast to the case of $\text{La}_{0.7}\text{Sr}_{0.3}\text{MnO}_3$ [10], in which the envelope of the infrared-active E_u mode drives a low-frequency 1.2-THz rotational E_g mode impulsively, the Jahn-Teller A_g mode has a higher frequency (15 THz) than the inverse 130-fs envelope of the mid-infrared pulse. Thus, in $\text{La}_{0.5}\text{Sr}_{1.5}\text{MnO}_4$, this A_g mode is driven adiabatically within the laser pulse duration toward its distorted position – too slow to be driven coherently.

In Figure 4, we present a caricature of the magnetic and orbital order melting process. Within the 130 fs timescale of the IRS-driven Jahn-Teller distortion, the equilibrium positions of both order parameters are rapidly quenched to a new value, i.e. the minimum of the free energy surface is displaced within the magnetic and orbital order parameter plane. After this prompt displacement, which we refer to as a *displacive exchange quench*, an effective force is exerted onto the spin and orbital degrees of freedom, driving relaxation toward the bottom of the new free energy surface.

The measured timescales for the two order parameters to settle to their new values are significantly

different from one another, with the orbital order approximately twice as fast for the same excitation fluence. Despite the complexity of the non-equilibrium relaxation process after the quench, a few considerations aid our understanding. The loss of orbital orientation involves only rearrangements in the e_g electrons, thus only one charge (or less) on each Mn^{3+} site, and no significant change in spin momentum *per se*. We expect this effect to occur more rapidly. On the other hand, the loss of antiferromagnetic spin order, for which one e_g and three t_{2g} spins rotate, requires a significant exchange of spin angular momentum, and thus has significant inertia.

The mechanism of this displacive exchange quench following nonlinear lattice excitation qualitatively explains the disordering of the system, although the microscopic pathway and the non-equilibrium physics at play are not clear. Also, the recovery of the disordered state to thermal equilibrium on longer time requires further clarification. An important effect to be understood is related to the coupling to other degrees of freedom after the exchange quench, including the fate of the angular momentum and the entropy increase that follows coupling to the thermodynamic bath. An important goal with great potential for applications would be to find routes to reverse the sign of the Jahn-Teller distortion with a second pulse after the magnetic and the orbital orders have relaxed into their new equilibrium values. This would only be possible if the coupling to the bath was small and the generation of entropy minimal.

In summary, we have shown that direct excitation of the lattice in a manganite using high intensity mid-infrared pulses melts the spin order, an effect that can only be measured directly using a direct femtosecond x-ray probe. We explain this process by considering the ionic Raman scattering mechanism and the excitation of the A_g Jahn-Teller motion through lattice nonlinearities, which is posited to lead to a displacive force on the spin and orbital order. Control of magnetism through

direct distortion of the lattice may, in appropriate excitation geometries, lend itself to bi-directional switching, of interest for high-speed data processing applications.

ACKNOWLEDGEMENT

The authors acknowledge stimulating conversations with S.B. Wilkins and R. Merlin.

This work was funded by the Max Planck Society through institutional support for the Max Planck Research Group for Structural Dynamics at the University of Hamburg. Portions of this research were carried out on the SXR Instrument at the Linac Coherent Light Source (LCLS), a division of SLAC National Accelerator Laboratory and an Office of Science user facility operated by Stanford University for the U.S. Department of Energy. The SXR Instrument is funded by a consortium whose membership includes the LCLS, Stanford University through the Stanford Institute for Materials Energy Sciences (SIMES), Lawrence Berkeley National Laboratory (LBNL), University of Hamburg through the BMBF priority program FSP 301, and the Center for Free Electron Laser Science (CFEL).

Work performed at Brookhaven was supported by US Department of Energy, Division of Materials Science under contract no. DE-AC02-98CH10886. Work at Argonne is supported under Contract No. DE-AC02-06CH11357 by UChicago Argonne, LLC, Operator of Argonne National Laboratory, a U.S. Department of Energy Office of Science Laboratory.

S. Wall acknowledges support from the Alexander von Humboldt Foundation.

FIGURE CAPTIONS

Fig. 1: (a) Top-view of the pump-probe scheme and scattering geometries for the orbital ($\frac{1}{4} \frac{1}{4} 0$) and the magnetic ($\frac{1}{4} \frac{1}{4} \frac{1}{2}$) diffraction peaks, measured on a (110) surface normal crystal of $\text{La}_{0.5}\text{Sr}_{1.5}\text{MnO}_4$. The Bragg planes are indicated as parallel lines; polarizations of the LCLS X-ray beam and the mid-infrared light are horizontal and vertical, respectively. Also shown are the energy dependencies measured at beamline X1A2, National Synchrotron Light Source. Panels (b) and (c) show the diffracted spots, recorded over 180×180 pixels of a fast CCD at LCLS. Images represent the average of 70 shots of the FEL.

Fig. 2: (a) Time-resolved changes of the intensity of the scattered X-ray spot at the magnetic ($\frac{1}{4} \frac{1}{4} \frac{1}{2}$) diffraction peak for vibrational excitation at $13.8 \mu\text{m}$ (mid-infrared) and photo-doping at 800 nm (near-infrared) pump wavelengths. Excitation fluences are 1.2 and 5 mJ/cm^2 , respectively. (b) Comparison of the melting of the orbital and magnetic order for 1.2-mJ/cm^2 mid-infrared excitation. The red lines are single exponential fits to the data, with time constants of 6.3 ps and 12.2 ps , respectively. (c) Transient change of the scattering angle 2θ and the width w of the diffracted x-ray spot measured for the magnetic wave vector following the mid-infrared excitation.

Fig. 3: (a) Schematic of charge and orbital order pattern in the ab -plane of $\text{La}_{0.5}\text{Sr}_{1.5}\text{MnO}_4$, together with the orbital order unit cell (thick light-blue line). Displacements of Mn and O atoms associated with (b) the resonantly driven IR-active B_{2u} mode and (c) the Raman-active A_g mode driven through *Ionic Raman scattering* are also shown. The latter mode relaxes the Jahn-Teller distortions to affect the exchange interaction.

Fig. 4: Excitation of the lattice reduces the Jahn-Teller distortion as in Figure 3(b), resulting in an effective shift in the equilibrium value of the orbital and magnetic order parameters. The effective force on each order parameter is given by the projection of the gradient along each axis.

REFERENCES

-
- [1] E. Beaurepaire, J.C. Merle, A. Daunois, and J.Y. Bigot, *Phys.Rev.Lett.* **76**, 4250 (1996).
- [2] A.V. Kimel, R.V. Pisarev, J. Hohlfeld, and T. Rasing, *Phys.Rev.Lett.* **89**, 287401 (2002).
- [3] C.D. Stanciu et al., *Phys. Rev. Lett.* **99**, 047601 (2007).
- [4] M. Matsubara et al., *Phys.Rev.Lett.* **99**, 207401 (2007).
- [5] S. Wall, D. Prabhakaran, A.T. Boothroyd, and A. Cavalleri, *Phys Rev. Lett.* **103**, 097402 (2009).
- [6] H. Ehrke et al., *Phys. Rev. Lett* **106.**, 217401 (2011).
- [7] M. Rini M. et al., *Nature* **449**, 72 (2007).
- [8] R.I. Tobey, D. Prabhakaran, A.T. Boothroyd, and A. Cavalleri, *Phys. Rev. Lett.* **101**, 197404 (2008).
- [9] D. Fausti et al., *Science* **331**, 189 (2011).
- [10] M. Först et al., *Nature Physics* advance online publication, 08 August 2011 (doi:10.1038/nphys2055).
- [11] H.Y. Hwang et al., *Phys. Rev. Lett.* **75**, 914 (1995).
- [12] H.Y. Hwang, T.T.M. Palstra, S.W. Cheong, and B. Batlogg, *Phys. Rev. B* **52**, 15046 (1995).
- [13] T. Kimura et al., *Nature* **426**, 55 (2003).
- [14] M. Fiebig, *Journal of Physics D* **38**, R123 (2005).
- [15] J. Wang et al., *Science* **299**, 1719 (2003).
- [16] J.B. Goodenough, *Phys.Rev.* **100**, 564 (1955).
- [17] B.J. Sternlieb et al., *Phys.Rev.Lett.* **76**, 2169 (1996).
- [18] D. Senff et al., *Phys. Rev. B* **77**, 184413 (2008).
- [19] J. van den Brink, G. Khaliullin, and D. Khomskii, *Phys. Rev. Lett.* **83**, 5118 (1999).
- [20] S.B. Wilkins et al., *Phys. Rev. Lett.* **91**, 167205 (2003).

-
- [21] S.S. Dhesi et al., *Phys. Rev. Lett.* **92**, 056403 (2004).
- [22] S.B. Wilkins et al., *Phys. Rev. B* **71**, 245102 (2005).
- [23] Staub U. et al. Charge/orbital ordering vs. Jahn-Teller distortion in $\text{La}_{0.5}\text{Sr}_{1.5}\text{MnO}_4$. *Europhys. Lett.* **76**, 926 (2006).
- [24] T. Ishikawa, K. Ookura, and Y. Tokura, *Phys. Rev. B* **59**, 8367 (1999).
- [25] P. Emma et al., *Nature Photonics* **4**, 641 (2010).
- [26] K. Holldack et al., *Appl. Phys. Lett.* **97**, 062502 (2010).
- [27] T. Ogasawara et al., *Phys. Rev. B* **63**, 113105 (2001).
- [28] R.D. Averitt et al., *Phys. Rev. Lett.* **87**, 017401 (2001).
- [29] H. Ogasawara et al., *Journ. Phys. Soc. Jpn* **69**, 1274 (2000).
- [30] We also analyzed the transient width and position of the magnetic diffraction peak for the near-infrared excitation. For the given excitation fluence, we do not observe a pump-induced change in position, either, but the calculated standard deviation for $\Delta(2\theta)/(2\theta)$ is only better than $< 3 \times 10^{-4}$ in this case. This value corresponds to a 50 K upper limit for the temperature increase induced by the 800 nm pulse.
- [31] R.F. Wallis and A.A. Maradudin, *Phys. Rev. B* **3**, 2063 (1971).
- [32] T.P. Martin and L. Genzel, *phys. stat. sol. (b)* **61**, 493 (1974).
- [33] P.G. Radaelli, D.E. Cox, M. Marezio, and S.W. Cheong, *Phys. Rev. B* **55**, 3015 (1997).
- [34] J.H. Hung, H.J. Lee, T.W. Noh, and Y. Moritomo, *J. Phys. Cond. Mat.* **12**, 9799 (2000).
- [35] K. Yamamoto et al., *Phys. Rev. B* **61**, 14706 (2000).

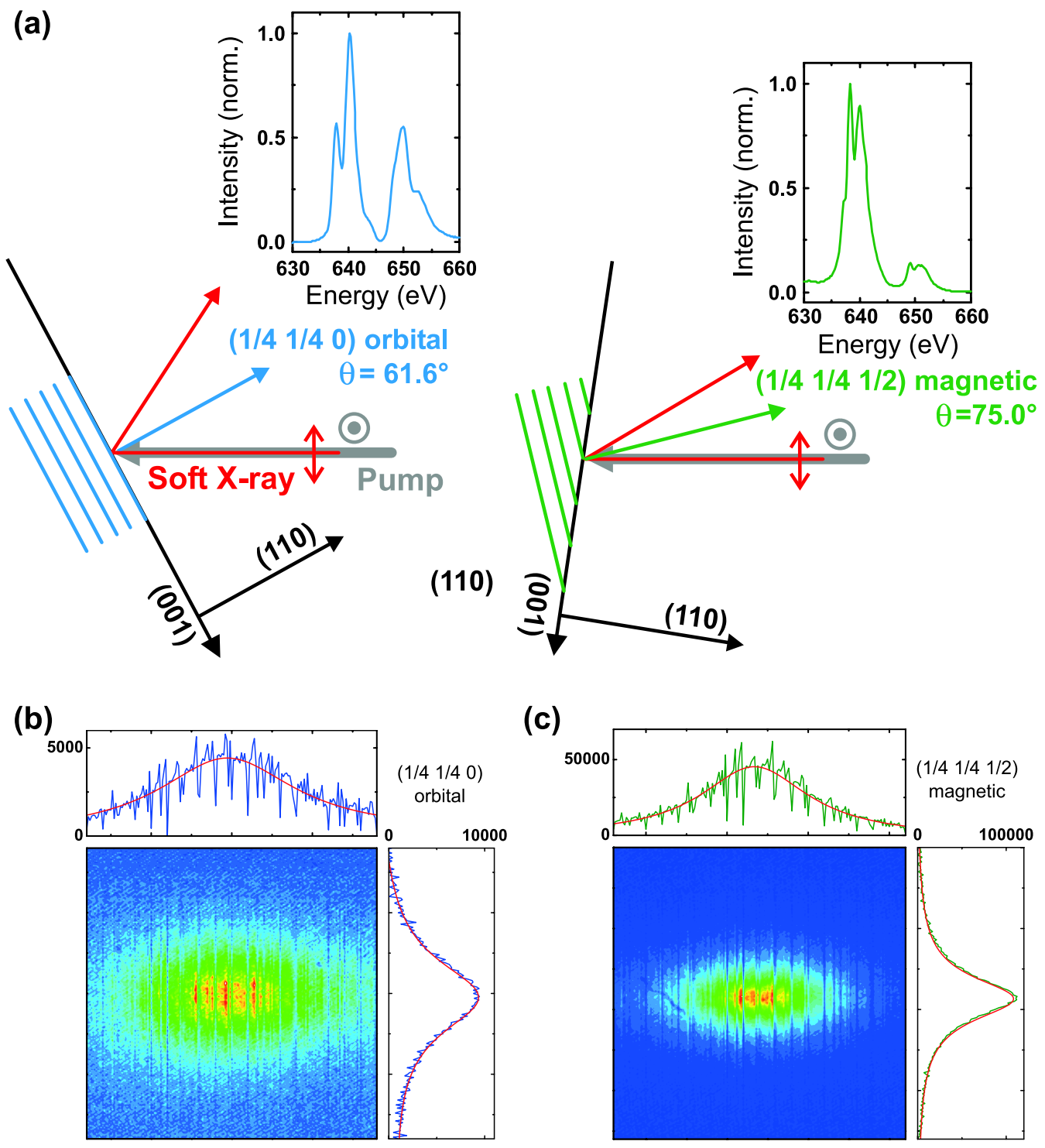


Figure 1 LF13551 10NOV2011

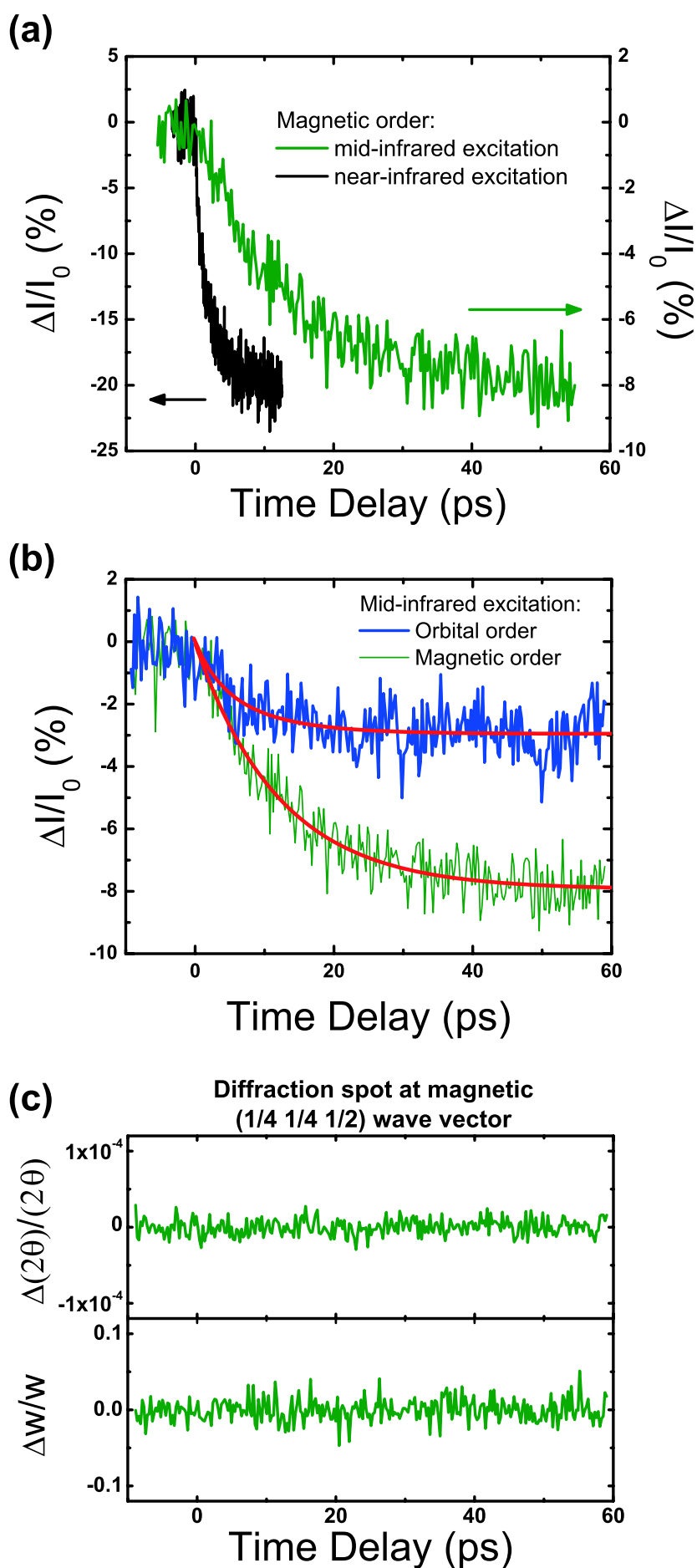


Figure 2 LF13551 10NOV2011

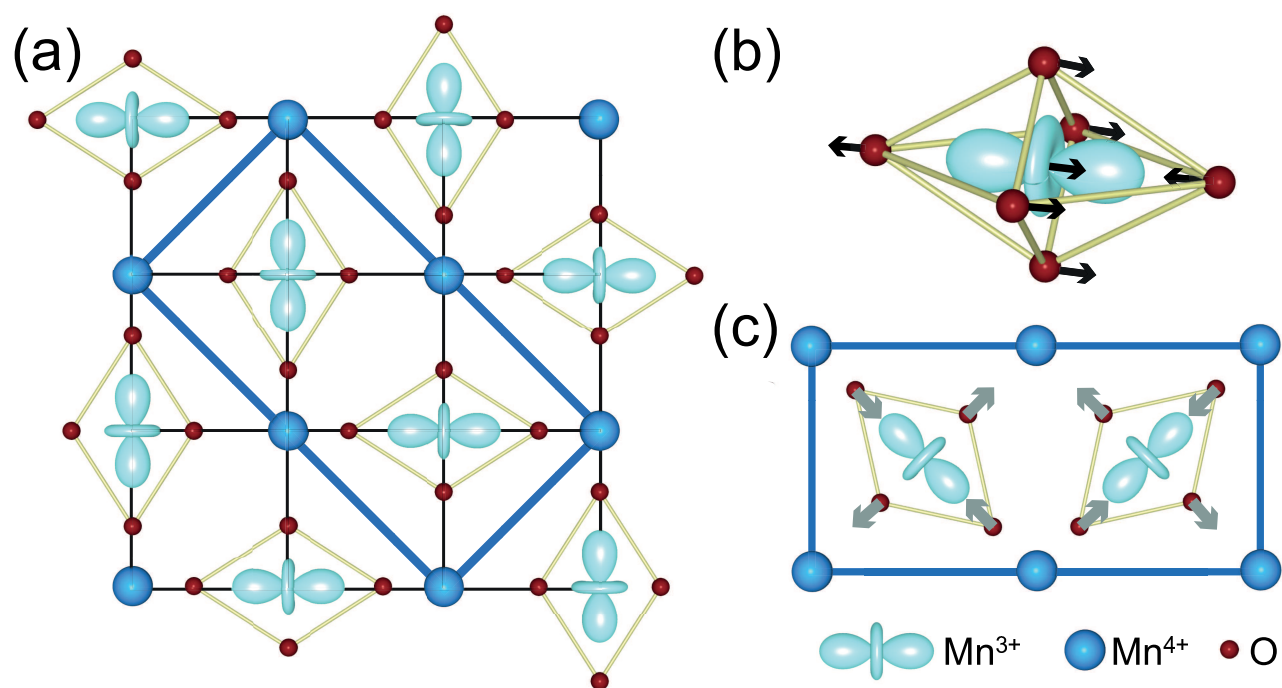


Figure 3

LF13551

10NOV2011

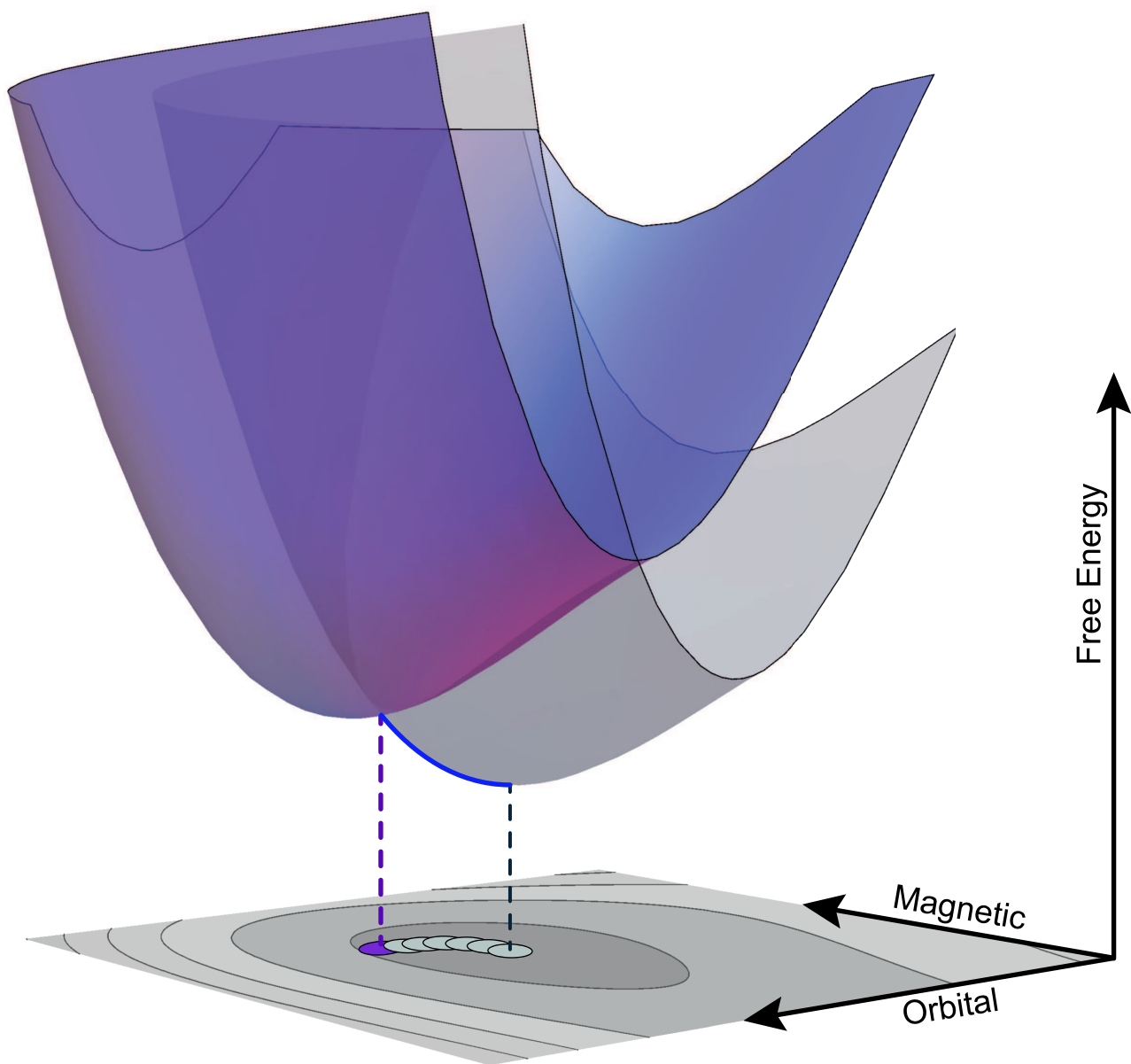


Figure 4

LF13551

10NOV2011